
MIT Open Access Articles

Optimal Charging Profiles with Minimal Intercalation-Induced Stresses for Lithium-Ion Batteries Using Reformulated Pseudo 2-Dimensional Models

The MIT Faculty has made this article openly available. ***Please share*** how this access benefits you. Your story matters.

Citation	Suthar, B., P. W. C. Northrop, R. D. Braatz, and V. R. Subramanian. “Optimal Charging Profiles with Minimal Intercalation-Induced Stresses for Lithium-Ion Batteries Using Reformulated Pseudo 2-Dimensional Models.” Journal of the Electrochemical Society 161, no. 11 (October 2, 2014): F3144–F3155.
As Published	http://dx.doi.org/10.1149/2.0211411jes
Publisher	Electrochemical Society
Version	Final published version
Accessed	Mon Apr 25 03:22:47 EDT 2016
Citable Link	http://hdl.handle.net/1721.1/101170
Terms of Use	Article is made available in accordance with the publisher's policy and may be subject to US copyright law. Please refer to the publisher's site for terms of use.
Detailed Terms	

MASSACHUSETTS INSTITUTE OF TECHNOLOGY

DSpace@MIT

NIH Public Access
Author Manuscript
Optim Control Appl Methods. Author manuscript; available in PMC 2014 November 01.

Published in final edited form as:
Optim Control Appl Methods. 2013 ; 34(6): 680–695. doi:10.1002/oca.2047.

Optimal Control of One-dimensional Cellular Uptake in Tissue Engineering†

Masako Kishida[1,2], **Ashlee N. Ford Versypt**[1], **Daniel W. Pack**[1], and **Richard D. Braatz**[2,*]
[1]University of Illinois at Urbana-Champaign, Urbana IL

[2]Massachusetts Institute of Technology, Cambridge, MA

SUMMARY

A control problem motivated by tissue engineering is formulated and solved in which control of the uptake of growth factors (signaling molecules) is necessary to spatially and temporally regulate cellular processes for the desired growth or regeneration of a tissue. Four approaches are compared for determining 1D optimal boundary control trajectories for a distributed parameter model with reaction, diffusion, and convection: (i) basis function expansion, (ii) method of moments, (iii) internal model control (IMC), and (iv) model predictive control (MPC). The proposed method-of-moments approach is computationally efficient while enforcing a non-negativity constraint on the control input. While more computationally expensive than methods (i)–(iii), the MPC formulation significantly reduced the computational cost compared to simultaneous optimization of the entire control trajectory. A comparison of the pros and cons of each of the four approaches suggests that an algorithm that combines multiple approaches is most promising for solving the optimal control problem for multiple spatial dimensions.

Keywords

Stem cell tissue engineering; Tissue engineering; Systems biology; Distributed parameter systems; Partial differential equations; Boundary control

1. INTRODUCTION

The primary goal of tissue engineering is the production of biological tissues for clinical use. One of the main manufacturing strategies utilizes the attachment or encapsulation of cells within a tissue matrix that is typically made of collagen or synthetic polymers [2, 3, 4]. Beyond receiving nutrients and releasing waste products, the development of a healthy functioning tissue requires that the cells uptake hormones, drugs, or signaling molecules in a controlled way [5, 6, 7, 8, 9, 10]. For example, in the development of tissues from stem cells, the stem cells must uptake growth factors, which are proteins that regulate cellular processes such as stimulating cellular proliferation and cell differentiation. The spatial and temporal control of the cellular uptake can be achieved through localized release (e.g., [11, 12, 13]).

Many materials and devices have been created for releasing molecules in a controlled way [14, 15]. Biodegradable polymeric nano- or microparticles have been developed that can be

†This paper is expanded version of previously presented conference paper [1].

Copyright ©2010 John Wiley & Sons, Ltd.

*Correspondence to: Massachusetts Institute of Technology, Room 66-372, 77 Massachusetts Avenue, Cambridge, MA 02139 USA, Phone: 617.253.3112, Fax: 617.258.0546, braatz@mit.edu.

NIH-PA Author Manuscript
NIH-PA Author Manuscript
NIH-PA Author Manuscript

NIH-PA Author Manuscript

NIH-PA Author Manuscript

NIH-PA Author Manuscript

placed within a tissue matrix to provide localized timed release. These particles include spheres, core-shell particles, and capsules that encapsulate small molecules, protein, or DNA including growth factors or other signalling molecules or, in the case of microcapsules, can contain cells that excrete hormones or other macromolecules. Techniques have been established to make highly uniform particles that produce a wide variety of highly reproducible release profiles by manipulating physical dimensions or by combining different types of particles [16, 17]. These particles can be accurately positioned and attached to a tissue matrix using such technologies as solid free-form fabrication [18] and layer-by-layer stereolithography [19], so as not to move until the particles have released their payloads to the cells.

The tissue engineering application motivates the formulation of an optimal control problem for the release of molecules from biodegradable polymeric nano- or microparticles to achieve a specified temporal and spatial uptake rate for cells within a tissue matrix. A potential application is to control the development of a tissue from stem cells within a matrix, so that the timed release of different growth factors in various locations form the multiple types of cells needed for the functioning components of a tissue. The shape and dimensions of these components are a function of both the spatial and temporal release of growth factors (e.g., [11]).

Tissue engineering with one spatial dimension arises when the growth factor is released at a surface to control the development of tissue within a fixed distance from that surface, such as would occur in the engineering of the epithelial tissue that forms the covering or lining of all internal and external body surfaces. This paper is the first (expect our previous conference paper [1]) to formulate tissue engineering as an optimal control problem. The paper compares several approaches to solving the optimal control problem for one spatial dimension to provide insights into how to best address the much more complicated case of three spatial dimensions, which would be required for more complicated organs such as a heart. Section 2 formulates molecular release within a biological tissue as a distributed parameter optimal control problem. Sections 3–6 solve the control problem using four methods: basis function expansion, method of moments, internal model control (IMC), and model predictive control. Finally, Section 7 provides a summary and recommendations on how to solve the optimal control problem with higher spatial dimensions.

2. PROBLEM SETUP

To keep the nomenclature consistent, the term *growth factor* will refer to the molecule being released, although the theory and algorithms also directly apply to other molecules such as drugs, hormones, and DNA for gene therapy. Spatial and temporal control of the cellular uptake rate in a biological tissue under the influence of reaction, diffusion and convection can be formulated as a distributed parameter optimal control problem:

$$\min_{u_j \in \mathcal{U}_j} \sum_j \int_0^{t_f} \int_V (J_{des,j}(x,y,z,t) - R_j(x,y,z,t))^2 dV dt, \quad (1)$$

where $J_{des,j}$ is the desired cellular uptake rate for species j, R_j is its cellular uptake rate, and its concentration C_j is the solution to the reaction-diffusion-convection equation [20]

$$\frac{\partial C_j}{\partial t} + v \cdot \nabla C_j = \nabla \cdot (D_j \nabla C_j) - R_j, \quad (2)$$

(x, y, z) are the spatial coordinates defined over domain V, t_f is the final time of interest, v is a known velocity field as a function of the spatial coordinates, and D_j is the effective

NIH-PA Author Manuscript

NIH-PA Author Manuscript

NIH-PA Author Manuscript

diffusion coefficient for species j. Depending on the specific tissue engineering application, the optimal control variables u_j, which influence the solution to partial differential equation (PDE) (2), can be either distributed throughout the spatial domain such as in the case that controlled release particles are integrated into the tissue matrix, or can be a subset $\mathcal{U}_j$ of the boundary conditions on the surface of the domain V. This model (2) considers applications in which the minimum length scales of interest in the domain V are larger than the maximum dimensions of the molecules, cells, and polymer particles that release growth factors. The cellular uptake kinetics and desired rate $J_{des,j}$ are determined in small-scale biological experiments so as to produce a response, such as differentiation to form a desired type of cell [5, 21, 20]. The model (2) is appropriate in the early stages of tissue development, before substantial cell migration and proliferation occur.

A standard approach to solving the above optimal control problem is the finite difference method, in which the control variable $u_j(x, y, z, t)$ and state $C_j(x, y, z, t)$ are discretized with respect to the spatial and time variables, inserted into (1)–(2), and solved numerically as an algebraic optimization problem. The difficulty in applying this approach using the standard discretization of the control and state (e.g., $C_j(x_k, y_l, z_m, t_n)$) is the large number of degrees of freedom. For example, for a single three-dimensional (3D) state, 100 discretization points in each spatial dimension and in time results in $100^4 = 10^8$ degrees of freedom in the algebraic optimization. The large dimensionality of such distributed parameter control problems is well recognized in the optimal control literature (e.g., [22, 23]). While many approaches have been proposed, no single algorithm dominates the literature or applications and it is generally accepted that the best approach depends on the details on the optimal control problem being solved.

To gain insight into how to best solve the 3D optimal control problem (1)–(2), this manuscript solves the 1D optimal control problem for a single species with manipulatable boundary condition and linear cellular uptake kinetics:

$$\min_{u(t)\geq 0} \int_0^{t_f} \left(J_{des}(t) - kC(1,t)\right)^2 dt \quad (3)$$

subject to the PDE

$$\frac{\partial C}{\partial t} + v\frac{\partial C}{\partial x} = D\frac{\partial^2 C}{\partial x^2} - kC, \forall x \in (0,1), \forall t > 0, \quad (4)$$

with initial and boundary conditions

$$C(x,0) = 0, \quad C(0,t) = u(t), \quad D\frac{\partial C}{\partial x}\bigg|_{x=1} = 0. \quad (5)$$

The reference trajectory $J_{des}(t) \geq 0$, $\forall t > 0$ is a desired cellular uptake rate at one boundary (at $x = 1$) and the control trajectory is the concentration $u(t)$ at the other boundary ($x = 0$) (see Fig. 1). The control input $u(t)$ is the concentration of growth factor, which is non-negative. This problem arises when the objective is to ensure that a desired time-varying uptake of a growth factor occurs at a specified distance (of 1 dimensionless unit) from a position where the growth factor is released through micro- or nanoparticles or is carried with fluid entering the tissue at $x = 0$ (this fluid also brings nutrients such as glucose to the cells). The cells within the domain would uptake at least as much growth factor as cells at $x = 1$, ensuring that all of the cells within the domain respond to the growth factor. The case

NIH-PA Author Manuscript

NIH-PA Author Manuscript

NIH-PA Author Manuscript

where too much cellular uptake of growth factor is undesirable can be handled by the incorporation of nanoparticles with the scaffold as in [24].

The following sections consider Gaussian reference trajectories, which have been employed in tissue engineering experiments [25, 26, 27, 28], and step trajectories that are useful for illustrating performance limitations associated with sharp changes in the desired cellular uptake profile. Any trajectory can be well approximated by a linear combination of Gaussian and step functions.

3. BASIS FUNCTION EXPANSION

This method generalizes an approach studied in the mid-1980s to solve optimal control problems for systems described by ordinary differential equations [23] to PDEs, in a similar manner as has been done for sheet and film processes (e.g., see [29, 30, 31], and citations therein) as well as nonlinear PDEs such as Burgers equation [22]. To apply this method, start with the analytical solution to the PDE (4) ([32]):

$$C(1,t)=e^{\frac{v}{2D}}D\sum_{n=1}^{\infty}\mu_n B_n \sin(\sqrt{\mu_n})\int_0^t u(\tau)e^{-(\frac{v^2}{4D}+k+\mu_n D)(t-\tau)}d\tau, \quad (6)$$

where

$$B_n=4\frac{\frac{v}{v+2D}\left(\frac{\sin\sqrt{\mu_n}}{\sqrt{\mu_n}}-\cos\sqrt{\mu_n}\right)-1+\cos\sqrt{\mu_n}}{2\sqrt{\mu_n}-\sin(2\sqrt{\mu_n})} \quad (7)$$

and μ_n is the nth root of

$$\tan\sqrt{\mu_n}=-2\sqrt{\mu_n}D/v. \quad (8)$$

Parameterize the control trajectory

$$u(t)\approx\sum_{i=1}^{n}a_i\varphi_i(t)=a^T\varphi(t), \quad (9)$$

in terms of any set of linearly independent basis functions $\{\phi_i(t)\}$, where

$$a=[a_1,a_2,\cdots,a_n]^T, \quad (10)$$

$$\varphi(t)=[\varphi_1(t),\varphi_2(t),\cdots,\varphi_n(t)]^T. \quad (11)$$

With $f_i(t)$ defined as the solution to the PDE (4) for the input $\phi_i(t)$,

$$f_i(t)=e^{\frac{v}{2D}}D\sum_{n=1}^{\infty}\mu_n B_n \sin(\sqrt{\mu_n})\int_0^t \varphi_i(\tau)e^{-(\frac{v^2}{4D}+k+\mu_n D)(t-\tau)}d\tau, \quad (12)$$

and

NIH-PA Author Manuscript

NIH-PA Author Manuscript

NIH-PA Author Manuscript

$$f(t)=[f_1(t), f_2(t), \cdots, f_n(t)]^T, \quad (13)$$

the optimal control problem with $u(t)$ parameterized by (9) can be written as

$$\min_{a^T\varphi(t)\geq 0} \int_0^{t_f} \left(J_{des}(t)-ka^T f(t)\right)^2 dt \quad (14)$$

as the function (6) is a linear operator on $u(t)$. While this approach does reduce the optimization over a function $u(t)$ to the optimization of a finite number of parameters a, the inequality constraint (14) remains defined over a continuum. The simplification occurs by dropping the non-negativity constraint on $u(t)$ to enable an approximate analytical solution to the optimal control problem to be obtained:

$$\frac{d}{da}\int_0^{t_f} \left(J_{des}^2(t)-2kJ_{des}(t)a^T f(t)+\left(ka^T f(t)\right)^2\right) dt=\int_0^{t_f} \left(-2kJ_{des}(t)f(t)+2k^2 f(t)f^T(t)a\right) dt=0, \quad (15)$$

$$\Rightarrow a=\tfrac{1}{k}\left(\int_0^{t_f} f(t)f^T(t)dt\right)^{-1}\int_0^{t_f} J_{des}(t)f(t)dt, \quad (16)$$

$$u(t)=\varphi^T(t)a=\tfrac{\varphi^T(t)}{k}\left(\int_0^{t_f} f(t)f^T(t)dt\right)^{-1}\int_0^{t_f} J_{des}(t)f(t)dt. \quad (17)$$

There are many choices of basis functions [29, 31] for which the temporal accuracy to the solution of the unconstrained optimal control problem is specified directly by the number of basis functions. A set of basis functions that provides excellent performance for one reference trajectory can give poor performance for another. For example, excellent tracking performance is obtained for a Gaussian reference trajectory, using 20 terms in a truncated Fourier cosine series [34] as the basis functions $\phi_i(t)$ (see Fig. 2a). On the other hand, this same set of basis functions (i) can have oscillations near discontinuities along the time axis due to the Gibbs phenomenon [35, 36], and (ii) does not take into account the non-negativity constraint on the control variable, which can result in constraint violations. Figure 2b shows both deficiencies for a step reference trajectory.

4. METHOD OF MOMENTS

While the method of moments has been widely applied for the solution of optimal control problems involving population balance models [37, 38], the approach has had little application to other control problems. An exception is its application to determine the control needed to bring a distributed parameter system with nonzero initial condition to quiescent conditions in the least time [39]. Here we present a new and different approach to applying method of moments to optimal control problems, that utilizes analytical expressions derived for the moments of the output variables in a PDE in terms of the moments of the input variables. For a linear system with u, tu, t^2u, y, ty, t^2y, g, tg, t^2g in L_1, the input and output are related by

$$\mu_y=\mu_g+\mu_u, \quad (18a)$$

NIH-PA Author Manuscript

NIH-PA Author Manuscript

NIH-PA Author Manuscript

$$\sigma_y^2=\sigma_g^2+\sigma_u^2, \quad (18b)$$

where μ_y is the mean residence time defined by

$$\mu_y=\frac{\int_0^\infty ty(t)dt}{\int_0^\infty y(t)dt}, \quad (19)$$

and σ_y^2 is the variance

$$\sigma_y^2=\frac{(\int_0^\infty t^2y(t)dt)\,(\int_0^\infty y(t)dt)-(\int_0^\infty ty(t)dt)^2}{(\int_0^\infty y(t)dt)^2}, \quad (20)$$

which is a measure of the spread of the function $y(t)$ about its mean; similar expressions hold for u and g. Equation (18b) can be proved using the Laplace transforms of the input ($U(s)$), output ($Y(s)$), and process ($Y(s) = G(s)U(s)$). First note that

$$(-1)^nU^{(n)}(0)=\int_0^\infty t^nu(t)dt \quad (21)$$

provided the integral exists [40],† where $U^{(n)}$ is the nth derivative of $U(s)$ with respect to s. Equation (18b) follows from (21) and application of the chain rule (see appendix).

When used together, equations (18b) and (21) enable the determination of the mean residence time and spread of the output of a linear system without analytical or numerical determination of $g(t)$ or $y(t)$. This property is especially useful for distributed parameter systems for which these functions are unknown, or are known but described by complicated infinite series. Analytical expressions can be derived for μ_g and σ_g directly from the Laplace transform of the PDE with respect to time, and μ_y and σ_y computed easily from (18b).

To illustrate these ideas, consider the transfer function obtained by taking the Laplace transform of (4) with respect to time, which gives

$$G(s)=\frac{kC(1,s)}{U(s)}=ke^{v/D}\frac{\xi_1-\xi_2}{\xi_1e^{\xi_1}-\xi_2e^{\xi_2}}, \quad (22)$$

where

$$\xi_1=\frac{v+\sqrt{v^2+4(k+s)D}}{2D}, \quad \xi_2=\frac{v-\sqrt{v^2+4(k+s)D}}{2D}. \quad (23)$$

From (21), exact analytical expressions for

†Existence is implied, for example, if the Laplace transform of the function $u(t)$ is analytic in the closed right-half plane.

NIH-PA Author Manuscript

NIH-PA Author Manuscript

NIH-PA Author Manuscript

$$\mu_g = -\frac{G^{(1)}(0)}{G(0)}, \quad \sigma_g = \sqrt{\frac{G^{(2)}(0)}{G(0)} - \left(\frac{G^{(1)}(0)}{G(0)}\right)^2} \quad (24)$$

are obtained from $G(s)$ using Mathematica or Maple. In contrast, the expressions for μ_g and σ_g derived in the time domain are more complicated. Insertion of $u(t) = \delta(t)$ into the analytical solution (6) results in

$$\mu_g = \frac{\int_0^\infty tC(1,t)dt}{\int_0^\infty C(1,t)dt} = \frac{\sum_{n=1}^{\infty} \frac{\mu_n B_n \sin\sqrt{\mu_n}}{(v^2/4D+k+\mu_n D)^2}}{\sum_{n=1}^{\infty} \frac{\mu_n B_n \sin\sqrt{\mu_n}}{v^2/4D+k+\mu_n D}} \quad (25)$$

$$\sigma_g^2 + \mu_g^2 = \frac{\int_0^\infty t^2 C(1,t)dt}{\int_0^\infty C(1,t)dt} = \frac{2\sum_{n=1}^{\infty} \frac{\mu_n B_n \sin\sqrt{\mu_n}}{(v^2/4D+k+\mu_n D)^3}}{\sum_{n=1}^{\infty} \frac{\mu_n B_n \sin\sqrt{\mu_n}}{v^2/4D+k+\mu_n D}}, \quad (26)$$

where each μ_n in (8) has to be solved iteratively.

While moments have been applied to the analysis of PDEs for decades [41], here we apply these expressions to obtain a highly computationally efficient algorithm for solving an optimal boundary control problem. The reference trajectory J_{des} is decomposed into a linear combination of nonnegative basis functions, each of which is parameterized by mean time $\mu_{y,i}$ and variance $\sigma_{y,i}^2$;

$$J_{des}(t) \approx \sum_{i=1}^{N} J_i(t), \text{ where } J_i(t) \geq 0, \quad (27)$$

and

$$\mu_{y,i} = \frac{\int_0^\infty tJ_i(t)dt}{\int_0^\infty J_i(t)dt}, \quad \sigma_{y,i}^2 = \frac{\int_0^\infty t^2 J_i(t)dt}{\int_0^\infty J_i(t)dt}, \quad i = 1, \cdots, N. \quad (28)$$

The form of the basis function is selected such that the shape of the optimal control trajectory ϕ_i is known and parameterized by mean time and variance that are computed from the known μ_g, σ_g, and (18b):

$$\mu_{\varphi,i} = \mu_{y,i} - \mu_g, \quad \sigma_{\varphi,i}^2 = \sigma_{y,i}^2 - \sigma_g^2. \quad (29)$$

The overall optimal control trajectory is computed by summing the optimal control trajectories corresponding to each of the basis functions, as in (9). This approach provides nearly perfect tracking for a Gaussian reference trajectory using Gaussian basis functions [33], for which the optimal control trajectories are Gaussian-like functions (see Fig. 3). This approach is computationally efficient for computing a non-negative optimal control trajectory, as the computation of the summations in (25) and (26), is cheap and the

NIH-PA Author Manuscript

NIH-PA Author Manuscript

NIH-PA Author Manuscript

computation of the parameters for the optimal control trajectries, (29), requires only two subtractions per Gaussian.

5. INTERNAL MODEL CONTROL

The analytical expressions derived for Internal Model Control (IMC) [42] apply to real-rational functions with time delay rather than to the irrational transfer function (22). One approach to deriving a real-rational transfer function for the PDE (4) starts by taking the Laplace transform of (6) to obtain

$$G(s)=e^{\frac{v}{2D}D}\sum_{n=1}^{\infty}\frac{\mu_n B_n \sin\sqrt{\mu_n}}{s+v^2/4D+k+\mu_n D}. \quad (30)$$

Even with a large number of terms in the summation, this transfer function can have very different high frequency behavior than the PDE (see Fig. 4). This observation is consistent with the more general observation that analytical solutions for PDEs can have very slow convergence, in which case the solution obtained from a finite number of terms can have poor accuracy [43].

Another approach to deriving a real-rational transfer function is to apply the second-order finite-difference method to discretize the spatial variable in (4) (Method Of Lines, MOL):

$$\frac{dC_i}{dt}=D\frac{C_{i+1}-2C_i+C_{i-1}}{(\Delta x)^2}-v\frac{C_{i+1}-C_{i-1}}{2\Delta x}-kC_i, \quad (31)$$

where each C_i is a concentration, which is a function of time, that corresponds to an equally spaced spatial location with grid spacing Δx, $C_1 = C(0, t)$, $C_n = C(1, t)$, and $C_{n+1} = C_{n-1}$. The state-space equations for the discretized system are

$$\begin{aligned}\frac{d}{dt}\begin{bmatrix}C_1\\C_2\\\vdots\\C_n\end{bmatrix}&=\left(\frac{D}{(\Delta x)^2}\begin{bmatrix}-2&1&0&\cdots&0\\1&-2&1&\ddots&\vdots\\0&\ddots&\ddots&\ddots&0\\\vdots&\ddots&1&-2&1\\0&\cdots&0&2&-2\end{bmatrix}-\frac{v}{2(\Delta x)}\begin{bmatrix}0&1&0&\cdots&0\\-1&0&1&\ddots&\vdots\\0&\ddots&\ddots&\ddots&0\\\vdots&\ddots&-1&0&1\\0&\cdots&0&0&0\end{bmatrix}-k\begin{bmatrix}1&0&\cdots&0\\0&\ddots&\ddots&\vdots\\\vdots&\ddots&\ddots&0\\0&\cdots&0&1\end{bmatrix}\right)\begin{bmatrix}C_1\\C_2\\\vdots\\C_n\end{bmatrix}\\&+\left(\frac{D}{(\Delta x)^2}+\frac{v}{2\Delta x}\right)\begin{bmatrix}1\\0\\\vdots\\0\end{bmatrix}u(t),\end{aligned} \quad (32)$$

NIH-PA Author Manuscript

NIH-PA Author Manuscript

NIH-PA Author Manuscript

$$y=kC(1,t)=\begin{bmatrix} 0 & \cdots & 0 & k \end{bmatrix}\begin{bmatrix} C_1 \\ C_2 \\ \vdots \\ C_n \end{bmatrix}. \quad (33)$$

The transfer function from $u(t)$ to $y(t) = kC(1, t)$ is

$$G_r(s)=C(sI-A)^{-1}B, \quad (34)$$

where

$$A=\begin{bmatrix} -\frac{2D}{(\Delta x)^2}-k & \frac{D}{(\Delta x)^2}-\frac{v}{2\Delta x} & 0 & \cdots & 0 \\ \frac{D}{(\Delta x)^2}+\frac{v}{2\Delta x} & -\frac{2D}{(\Delta x)^2}-k & \ddots & \ddots & \vdots \\ 0 & \ddots & \ddots & \ddots & 0 \\ \vdots & \ddots & \frac{D}{(\Delta x)^2}+\frac{v}{2\Delta x} & \ddots & \frac{D}{(\Delta x)^2}-\frac{v}{2\Delta x} \\ 0 & \cdots & 0 & \frac{2D}{(\Delta x)^2} & -\frac{2D}{(\Delta x)^2}-k \end{bmatrix}, \quad (35)$$

$$B=\begin{bmatrix} \frac{D}{(\Delta x)^2}+\frac{v}{2\Delta x} \\ 0 \\ \vdots \\ 0 \end{bmatrix}, \quad C=\begin{bmatrix} 0 & \cdots & 0 & k \end{bmatrix}. \quad (36)$$

This approximate transfer function for the PDE is accurate over the frequency range of the interest, even with a coarse spatial discretization (see Bode plots in Fig. 4).

The real-rational transfer function (34) is minimum phase, for which the IMC controller is [42]

$$Q(s)=F(s)/G_r(s), \text{ where } F(s)=\frac{1}{(\lambda s+1)^n} \quad (37)$$

and λ is the IMC tuning parameter. Applications of IMC for Gaussian and step reference trajectories are shown in Fig. 5. The value of λ was set just large enough for the control variable to be nonnegative. This approach can give insight into the form of the optimal control trajectory, but is suboptimal and does not handle general constraints; extensions of IMC to handle constraints [44] are not optimal with respect to the optimization objective (3).

6. MODEL PREDICTIVE CONTROL

Model predictive control (MPC) is a well-known method for solving optimal control problems with constraints [45] that has been applied to distributed parameter systems in industry since the late 1970s [46]. Since the early 1990s, many researchers have proposed the application of MPC to lumped parameter models for distributed parameter systems in which the actuation is distributed along a physical boundary (e.g., see [31] and citations therein). Very few papers have considered MPC implementations based on more sophisticated models of distributed parameter systems. Most closely related to this

NIH-PA Author Manuscript

NIH-PA Author Manuscript

NIH-PA Author Manuscript

application, [47, 48] developed an unconstrained MPC formulation that exploits the special characteristics of convection-dominated processes, whereas [49] applied a rather modern state-space MPC formulation to a model similar to (4).

In contrast to the usual application of MPC to closed-loop control problems, here MPC is used to solve an open-loop optimal control problem. Also, many MPC formulations assume a staircase control trajectory [50, 51]. To achieve a continuous control trajectory, the input-output process model was augmented by an integrator and the actual control variable was computed from the integral of the MPC control variable. This MPC formulation is a modification of a standard state-space formulation [52].

6.1. MPC Setup

The control trajectory in the tissue engineering application is better modeled as being continuous, which is much more accurately represented by a piecewise-linear rather than the staircase function usually used in MPC formulations. A piecewise-linear function can be implemented by augmenting the process input with an integrator, where u_a is a staircase function. The resulting PDE can be spatially and temporally discretized using the finite-difference method, which is equivalent to converting the continuous-time model of $G_r(s)/s$ into discrete time, to obtain the state-space model

$$x_a(h+1)=A_a x_a(h)+B_a u_a(h), \quad y(h)=C_a x_a(h), \quad (38)$$

where x_a is the state vector with an integrator and u_a is the control variable for the augmented system (its integral is u). The value for u_a at time instant h is obtained by solving the optimization:

$$\min_{\Delta u_a(h|h),\ldots,\Delta u_a(h+m-1|h)} \sum_{i=1}^{P} |y(h+i|h)-r(h+i)|^2 \quad (39)$$

subject to

$$\Delta u_a(h+i|h)=0, \quad i=m,\ldots,p-1, \quad (40)$$

$$\int_0^t u_a(\tau)d\tau=u(t)\geq 0, \quad (41)$$

where

$$\Delta u_a(h) \equiv u_a(h)-u_a(h-1), \quad (42)$$

p is the prediction horizon, m is the control horizon, $\Delta u_a(h)$ is the control increment, and "$(h + i|h)$" is the value predicted for time instant $h + i$ based on the information available at time instant h, and $r(h)$ is the reference variable J_{des} at time instant h. At time instant h, the piecewise-linear control trajectory

$$u(t)=\int_0^t u_a(\tau)d\tau \quad (43)$$

NIH-PA Author Manuscript

NIH-PA Author Manuscript

NIH-PA Author Manuscript

is implemented on the process, where $u_a(h) = u_a(h-1) + \Delta u_a(h|h)^*$ and $\Delta u_a(h|h)^*$ is the first element of the optimal sequence. The above process is repeated at each sampling instant based on the updated variables.

6.1.1. Prediction—From (38) the prediction at time instant h of the future output trajectory is

$$\begin{bmatrix} y(h+1) \\ \vdots \\ y(h+p) \end{bmatrix} = S_x x(h) + S_{u1} u(h-1) + S_u \begin{bmatrix} \Delta u_a(h) \\ \vdots \\ \Delta u_a(h+p-1) \end{bmatrix}, \quad (44)$$

where

$$S_x = \begin{bmatrix} C_a A_a \\ C_a A_a^2 \\ \vdots \\ C_a A_a^p \end{bmatrix}, \quad S_{u1} = \begin{bmatrix} C_a B_a \\ C_a B_a + C_a A_a B_a \\ \vdots \\ \sum_{j=1}^{p} C_a A_a^{j-1} B_a \end{bmatrix}, \quad (45)$$

$$S_u = \begin{bmatrix} C_a B_a & 0 & \cdots & 0 \\ C_a B_a + C_a A_a B_a & C_a B_a & \ddots & \vdots \\ \vdots & \vdots & \ddots & 0 \\ \sum_{j=1}^{p} C_a A_a^{j-1} B_a & \sum_{j=1}^{p-1} C_a A_a^{j-1} B_a & \cdots & C_a B_a \end{bmatrix}. \quad (46)$$

6.1.2. Optimization Variables—Equation (44) relates p outputs $y(h+1|h), \ldots, y(h+p|h)$ and p inputs $\Delta u_a(h|h), \ldots, \Delta u_a(h+p-1|h)$, while only m free optimization variables $\Delta u_a(h), \ldots, \Delta u_a(h+m-1)$ are available. With the optimization variables defined as $z(h+i) := \Delta u_a(h+i)$ for $i = 0, \ldots, m-1$ the last vector of (44) is related to the vector z by

$$\begin{bmatrix} \Delta u_a(h) \\ \vdots \\ \Delta u_a(h+p-1) \end{bmatrix} = M \begin{bmatrix} z(h) \\ \vdots \\ z(h+m-1) \end{bmatrix}, \quad (47)$$

where

$$M = \begin{bmatrix} I_m \\ 0_{(p-m)\times m} \end{bmatrix}. \quad (48)$$

6.1.3. Objective Function—The MPC objective (39) can be written in terms of z as

NIH-PA Author Manuscript

NIH-PA Author Manuscript

NIH-PA Author Manuscript

$$J(z)=\left\|\begin{bmatrix} y(h+1) \\ \vdots \\ y(h+p) \end{bmatrix}-\begin{bmatrix} r(h+1) \\ \vdots \\ r(h+p) \end{bmatrix}\right\|_2^2$$
$$=z^T K_{\Delta u} z+2\left(K_x x(h)+K_u u(h-1)+\begin{bmatrix} r(h+1) \\ \vdots \\ r(h+p) \end{bmatrix}^T K_r\right) z+\left\|S_x x(h)+S_{u1} u(h-1)-\begin{bmatrix} r(h+1) \\ \vdots \\ r(h+p) \end{bmatrix}\right\|_2^2, \quad (49)$$

where

$$K_{\Delta u}=M^T S_u^T S_u M, \quad K_r=-S_u M,$$
$$K_u=S_{u1}^T S_u M, \quad K_x=S_x^T S_u M.$$

6.1.4. Constraints—Satisfying (41) requires that $u(i) \geq 0$ for all $i = h + 1, \ldots, h + p$, which can be written as

$$\Delta t \begin{bmatrix} 1 & 0 & \cdots & 0 \\ 2 & \ddots & \ddots & \vdots \\ \vdots & \ddots & \ddots & 0 \\ p & \cdots & 2 & 1 \end{bmatrix} \begin{bmatrix} \Delta u_a(h) \\ \vdots \\ \Delta u_a(h+p-1) \end{bmatrix} \geq -\begin{bmatrix} 1 \\ \vdots \\ 1 \end{bmatrix} u(h)-\Delta t \begin{bmatrix} 1 \\ \vdots \\ p \end{bmatrix} u_a(h-1), \quad (50)$$

where Δt is the sampling time. Insertion of (47) results in the expression in terms of z.

6.1.5. MPC Simulation Results—The convex quadratic program (49)–(50) was solved at each time instant h by using the *qpdantz* implementation of the Dantzig-Wolfe algorithm in the Matlab Model Predictive Control toolbox [52]. The MPC formulation gave good reference tracking with a control horizon of $m = 2$ and a prediction horizon of $p = 3$, 5, or 7 for the sampling time of 1/10 (see Fig. 6).

6.2. Computational Requirements

The computational cost of MPC is an important consideration when extending this approach to a larger number of spatial dimensions (1)–(2). The computational cost for solving (49)–(50) is a linear or cubic function of the horizons, depending on the details of the numerical implementation [53, 54, 55, 56]. For implementations with a cubic cost dependency, the number of flops required for the MPC computation ($O(m^3)T$) is orders of magnitude lower than for simultaneous optimization of (3) over of the entire time period ($O((mT)^3)$), whre m is the control horizon and T is the number of time step. For implementations with a linear cost dependency, the MPC approach is similar to simultaneous optimization. More importantly, the MPC implementation with small horizons requires orders-of-magnitude less memory, which is an important consideration for a PDE model with three spatial dimensions.

The 1D optimal control problem is simple enough that simultaneous optimization could be implemented, by choosing m and p to span the entire length of the reference trajectory and dropping the use of the receding horizon. A regularization term of $10^{-4}I$ was added to $K_{\Delta u}$ in the optimization objective (39) to remove numerical ill-conditioning that arose due to the large number of degrees of freedom. The time-domain plots were very similar to those

NIH-PA Author Manuscript

NIH-PA Author Manuscript

NIH-PA Author Manuscript

obtained from the best MPC tuning (in Fig. 6), with the total computational cost for both approaches being about 0.1 second as measured by averaging the computation time on an Intel Core Duo computer over 10 trials measured using the Matlab program *tic-toc*.‡ Applying MPC to the optimal control problem resulted in nearly globally optimal results, with many orders-of-magnitude reduction in memory requirements. This suggests that MPC is suitable for the solution of the optimal control problem (1) for a larger number of spatial dimensions.

7. IMPLEMENTATION

From a practical point of view, the growth factor concentration at a boundary can be implemented by using a permeable or semipermeable membrane with an aqueous solution on the side opposite of the biological tissue. An increase in the growth factor concentration specified by solution of the optimal control problem can be physically implemented using a syringe pump that adds a small quantity of aqueous solution with a high concentration of growth factor, with the quantity at each sampling instance specified by a concentration measurement obtained by any spectroscopic method such as Fourier transform infrared spectroscopy [57]. A decrease in the growth factor concentration specified by solution of the optimal control problem can be physically implemented by dilution using another syringe pump, based on the same concentration measurement. When the optimal control problem is formulated so that the growth factor is released from within the tissue, the release can be either directly from the scaffold material or by polymeric nanoparticles adhered to the scaffold (see references in the Introduction). Such technologies are already described in some detail in the tissue engineering and related literatures, which include methods for precise positioning of the nanoparticles as well as cells within the scaffold during its construction [18, 19] while maintaining a high survival rate for the cells. The tissue engineering technologies for implemented such optimal control trajectories have been available for the last 5 years; what this paper considers is the design of systematic approach for determining how much growth factor should be released, instead of the current approach which is to use trial-and-error experimentation. Given the uncertainties of biological systems, implementation of optimal control methods may not produce the desired engineering tissue and organ exactly to specifications, but it is hoped that the proposed approaches are at least able to reduce the amount of experiments needed to develop a successful experimental protocol.

8. CONCLUSIONS

The strengths and weaknesses of four approaches were investigated for the solution of an optimal control problem motivated by tissue engineering. The basis function expansion approach is computationally efficient but can violate the non-negativity constraint on the control input and could lead to oscillations at discontinuities (see Fig. 2b), depending on the selection of basis functions and the reference trajectory. Basis functions that have been applied to other distributed parameter systems with convection and diffusion [29, 31] may have promise in this particular application. The internal model control method does not take constraints explicitly into account when optimizing the control objective, and detuning the IMC tuning parameter to satisfy the non-negativity constraint led to sluggish performance compared to the method-of-moments approach (compare Figs. 3 and 5a).

The new optimal control method based on the method of moments was highly computationally efficient while enforcing the non-negativity constraint on the control trajectory (see Fig. 3). While providing higher performance than IMC for a smooth reference

‡The total computational cost for MPC could be reduced by using warm starting [53, 54].

NIH-PA Author Manuscript

NIH-PA Author Manuscript

NIH-PA Author Manuscript

trajectory, it is unclear how to best generalize the approach to deal with state constraints or reference trajectories with discontinuities. The MPC approach was the most flexible method, with the ability to handle control and state constraints, but was also the most computationally expensive. Some results were presented that are of broader interest to the optimal control field:

1. the proposed method-of-moments approach to solving optimal control problems is different from and goes beyond its applications to population balance models,
2. MPC is shown to be a useful approach for solving some *non*-receding horizon optimal control problems (in particular, problems in which nearly optimal performance is obtained for a small control horizon).

The paper considered many approaches to solving the optimal control problem for one spatial dimension, to provide insights into how to best address the much more complicated case of three spatial dimensions. Recall that the 3D control problem (1)–(2) has too many degrees of freedom to be solved by direct temporal and spatial discretization. The results in Sections 3–6 suggest that the 3D optimal control problem may be solvable by a combination of multiple design methods. The generality and near optimality of MPC observed in Section 3 suggests that MPC is promising for solving the 3D control problem (1)–(2). The near optimality of the basis function expansion approach in Section 3 suggests that parameterization of the control input in terms of basis functions within such a 3D MPC algorithm would lead to minimal loss in performance for some reference trajectories while further reducing the computational time. The good suboptimal solution obtained by the method-of-moments approach motivates the development of 3D extensions to provide warm starts for a 3D MPC optimization, to speed convergence. Nonlinear uptake kinetics could be addressed by successive solution of linearized problems, just as nonlinear MPC problems are typically solved as a series of linearized MPC problems [58]. While how to best combine the various methods may depend on the spatial and temporal dependencies of the desired cellular uptake rate and how far an unconstrained solution is from satisfying the constraints, this conclusions section provides guidance as to the most promising method to incorporate depending on the needs of a particular application.

Acknowledgments

Support is acknowledged from the National Institutes of Health NIBIB 5RO1EB005181, a U.S. Department of Energy Computational Science Graduate Fellowship, and the Institute for Advanced Computing Applications and Technologies.

References

1. Kishida, M.; Ford, AN.; Pack, DW.; Braatz, RD. Optimal control of cellular uptake in tissue engineering. Proc. of the American Control Conference; Piscataway, NJ: IEEE Press; 2008. p. 2118-2123.
2. Bianco P, Robey PG. Stem cells in tissue engineering. Nature. 2001; 414(6859):118–121. [PubMed: 11689957]
3. Lee J, Cuddihy MJ, Kotov NA. Three-dimensional cell culture matrices: State of the art. Tissue Engineering B. 2008; 14:61–86.
4. Kim J, Yaszemski MJ, Lu L. Three-dimensional porous biodegradable polymeric scaffolds fabricated with biodegradable hydrogel porogens. Tissue Engineering C. 2009; 15:583–594.
5. Beaty CE, Saltzman WM. Controlled growth-factor delivery induces differential neurite outgrowth in 3-dimensional cell-cultures. J of Controlled Release. 1993; 24:15–23.
6. Langer R. Perspectives: Drug delivery - drugs on target. Science. 2001; 293(5527):58–59. [PubMed: 11441170]

NIH-PA Author Manuscript

NIH-PA Author Manuscript

NIH-PA Author Manuscript

7. Mikos AG, Herring SW, Ochareon P, Elesseeff J, Lu HH, Kandel R, Schoen FJ, Toner M, Mooney D, Atala A, et al. Engineering complex tissues. Tissue Engineering. 2006; 12:3307–3339. [PubMed: 17518671]
8. Cao L, Mooney DJ. Spatiotemporal control over growth factor signaling for therapeutic neovascularization. Advanced Drug Delivery Reviews. 2007; 59:1340–1350. [PubMed: 17868951]
9. Silva EA, Mooney DJ. Spatiotemporal control of vascular endothelial growth factor delivery from injectable hydrogels enhances angiogenesis. J Thromb Haemost. 2007; 5:590–598. [PubMed: 17229044]
10. Discher DE, Mooney DJ, Zandstra PW. Growth factors, matrices, and forces combine and control stem cells. Science 2009. 2009; 324(5935):1673–1678.
11. Shah NM, Anderson DJ. Integration of multiple instructive cues by neural crest stem cells reveals cell-intrinsic biases in relative growth factor responsiveness. PNAS. 1997; 94:11 369–11 374. [PubMed: 8990152]
12. Chan G, Mooney DJ. New materials for tissue engineering: Towards greater control over the biological response. Trends in Biotechnology. 2008; 28:382–392. [PubMed: 18501452]
13. Tayalia P, Mooney DJ. Controlled growth factor delivery for tissue engineering. Advanced Materials. 2009; 21:3269–3285. [PubMed: 20882497]
14. Langer R. Drug delivery and targeting. Nature. 1998; 392(6679):5–10. Suppl S. [PubMed: 9579855]
15. Saltzman, WM. Drug Delivery - Engineering Principles for Drug Therapy. Oxford University Press; Oxford, UK: 2001.
16. Berkland C, Cox A, Kim K, Pack DW. Three-month, zero-order piroxicam release from monodispersed double-walled microspheres of controlled shell thickness. J of Biomedical Materials Research Part A. 2004; 70A:576–584.
17. Varde NK, Pack DW. Microspheres for controlled release drug delivery. Expert Opinion on Biological Therapy. 2004; 4:35–51. [PubMed: 14680467]
18. Cima, LG.; Cima, MJ. Tissue regeneration matrices by solid free form fabrication techniques 1996. U.S. Patent #5,518,680.
19. Mapili G, Lu Y, Chen SC, Roy K. Laser-layered microfabrication of spatially patterned functionalized tissue-engineering scaffolds. J of Biomedical Materials Research Part B-Applied Biomaterials. 2005; 75B:414–424.
20. Truskey, GA.; Yuan, F.; Katz, DF. Transport Phenomena in Biological Systems. Prentice Hall; Upper Saddle River, NJ: 2004.
21. Langer R, Vacanti JP. Tissue engineering. Science. 1993; 260(5110):920–926. [PubMed: 8493529]
22. Kucuk I, Sadek I. An efficient computational method for the optimal control problem for the Burgers equation. Mathematical & Computer Modelling. 2006; 44:973–982.
23. Razzaghi M, Tahai A, Arabshahi A. Solution of linear 2-point boundary-value problems via Fourier-series and application to optimal-control of linear systems. J of the Franklin Institute. 1989; 326:523–533.
24. Kishida, M.; Braatz, RD. State-constrained optimal spatial field control for controlled release in tissue engineering. Proc. of the American Control Conference; Piscataway, NJ: IEEE Press; 2010. p. 4361-4366.
25. Raiche AT, Puleo DA. Cell responses to bmp-2 and igf-i released with different time-dependent profiles. J Biomed Mat Res Pt A. 2004; 69A:342–350.
26. Raiche AT, Puleo DA. In vitro effects of combined and sequential delivery of two bone growth factors. Biomaterials. 2004; 25:677– 685. [PubMed: 14607506]
27. Lee K, Silva EA, Mooney DJ. Growth factor delivery-based tissue engineering: general approaches and a review of recent developments. J R Soc Interface. 2010; 8:153–170. [PubMed: 20719768]
28. Chen FM, Zhang M, Wu ZF. Toward delivery of multiple growth factors in tissue engineering. Biomaterials. 2010; 31:6279–6308. [PubMed: 20493521]
29. Duncan, SR.; Heath, WP.; Halouskova, A.; Karny, M. Application of basis functions to the cross-directional control of web processes. Proc. of the UKACC Int. Conf. on Control ’96; Stevenage, England: IEE; 1996. p. 1278-1283.

NIH-PA Author Manuscript

NIH-PA Author Manuscript

NIH-PA Author Manuscript

30. Featherstone AP, Braatz RD. Control-oriented modeling of sheet and film processes. AIChE J. 1997; 43:1989–2001.
31. Featherstone, AP.; VanAntwerp, JG.; Braatz, RD. Identification and Control of Sheet and Film Processes. Springer Verlag; London: 2000.
32. Haberman, R. Applied partial differential equations. Prentice Hall; Upper Saddle River, NJ: 2003.
33. de Moivre, A. The Doctrine of Chances. 2. H. Woodfall; London: 1738.
34. Fourier, J. Thorie Analytique de la Chaleur. Académie des Sciences; Paris, France: 1822.
35. Gibbs JW. Fourier series. Nature. 1898; 59:200.
36. Wilbraham H. On a certain periodic function. Cambridge & Dublin Math J. 1848; 3:198–201.
37. Braatz RD. Advanced control of crystallization processes. Annual Reviews in Control. 2002; 26:87–99.
38. Rawlings JB, Miller SM, Witkowski WR. Model identification and control of solution crystallization processes: A review. Ind Eng Chem Res. 1993; 32:1275–1296.
39. Butkovsky, A. Distributed Control System. Elsevier; Amsterdam: 1969.
40. Aris R. On the dispersion of linear kinematic waves. Proc R Soc London A. 1958; 245:268–277.
41. Aris R. On the dispersion of a solute in a fluid flowing through a tube. Proc R Soc London, Ser A. 1956; 235:67–77.
42. Morari, M.; Zafiriou, E. Robust Process Control. Prentice Hall; Upper Saddle River, NJ: 1989.
43. Deen, WM. Analysis of Transport Phenomena. Oxford University Press; Oxford, UK: 1998.
44. Zheng A, Kothare MV, Morari M. Anti-windup design for internal model control. Int J of Control. 1994; 60:1015–1024.
45. Lee JH, Morari M, Garcia CE. State-space interpretation of model predictive control. Automatica. 1994; 30:707–717.
46. Prett, DM.; Ramakar, BL.; Cutler, CR. Dynamic matrix control process 1982. U.S. Patent #80,966. 1979. filed in
47. Shang H, Forbes JF, Guay M. Model predictive control for quasilinear hyperbolic distributed parameter systems. Ind Eng Chem Res. 2004; 43:2140–2149.
48. Shang H, Forbes JF, Guay M. Computationally efficient model predictive control for convection dominated parabolic systems. J of Process Control. 2007; 17:379–386.
49. Patwardhana AA, Wright GT, Edgar TF. Nonlinear model-predictive control of distributed-parameter systems. Chem Eng Sci. 1992; 47:721–735.
50. Camacho, EF.; Bordons, C. Model predictive control. Springer; London: 2004.
51. Garcia CE, Prett DM, Morari M. Model predictive control: Theory and practice - a survey. Automatica. 1989; 25:335–348.
52. Bemporad, A.; Morari, M.; Ricker, NL. Model Predictive Control Toolbox for Use with MATLAB: User's Guide. The Mathworks Inc; Natick, MA: 2004.
53. Bartlett RA, Biegler LT, Backstromb J, Gopal V. Quadratic programming algorithms for large-scale model predictive control. J of Process Control. 2002; 12:775–795.
54. Cannon M, Liao W, Kouvaritakis B. Efficient MPC optimization using Pontryagins minimum principle. Int J of Robust & Nonlinear Control. 2008; 18:831–844.
55. Rao CV, Wright SJ, Rawlings JB. Application of interior-point methods to model predictive control. JOTA. 1998; 99:723–757.
56. Vandenberghe, L.; Boyd, S.; Nouralishahi, M. Robust linear programming and optimal control. Proc. of the 15th IFAC World Congress on Automatic Control; 2002. p. 271-276.
57. Togkalidou T, Tung HH, Sun Y, Andrews A, Braatz RD. Solution concentration prediction for pharmaceutical crystallization processes using robust chemometrics and atr ftir spectroscopy. Org Process Res Dev. 2002; 6:317–322.
58. Lee YI, Kouvaritakis B, Cannon M. Constrained receding horizon predictive control for nonlinear systems. Automatica. 2002; 38:2093–2102.

NIH-PA Author Manuscript

NIH-PA Author Manuscript

NIH-PA Author Manuscript

A. DERIVATION OF EQUATION (18B)

$$\begin{aligned}\mu_y &= \frac{\int_0^\infty t y(t)dt}{\int_0^\infty y(t)dt} = \frac{-Y^{(1)}(0)}{Y(0)} \\ &= \frac{-G^{(1)}(0)U(0) - G(0)U^{(1)}(0)}{G(0)U(0)} \\ &= -\frac{G^{(1)}(0)}{G(0)} - \frac{U^{(1)}(0)}{U(0)} \\ &= \mu_g + \mu_u,\end{aligned} \tag{51}$$

$$\begin{aligned}\sigma_y^2 + \mu_y^2 &= \frac{\int_0^\infty t^2 y(t)dt}{\int_0^\infty y(t)dt} = \frac{Y^{(2)}(0)}{Y(0)} \\ &= \frac{G^{(2)}(0)U(0) + 2G^{(1)}(0)U^{(1)}(0) + U^{(2)}(0)G(0)}{G(0)U(0)} \\ &= \frac{G^{(2)}(0)}{G(0)} + 2\frac{G^{(1)}(0)}{G(0)}\frac{U^{(1)}(0)}{U(0)} + \frac{U^{(2)}(0)}{U(0)} \\ &= \sigma_g^2 + \mu_g^2 + 2\mu_g\mu_u + \sigma_u^2 + \mu_u^2,\end{aligned} \tag{52}$$

which implies (18b), after application of (51).

NIH-PA Author Manuscript

NIH-PA Author Manuscript

NIH-PA Author Manuscript

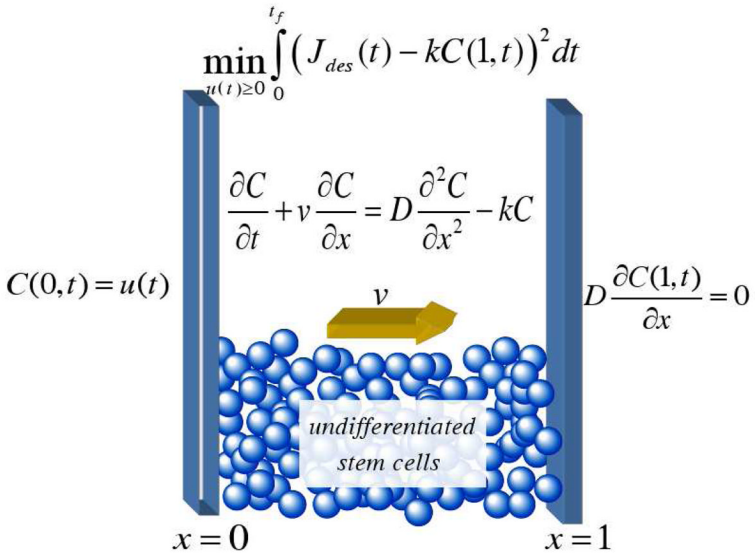

Figure 1.
Boundary control at $x = 0$ with a Neumann boundary condition at $x = 1$.

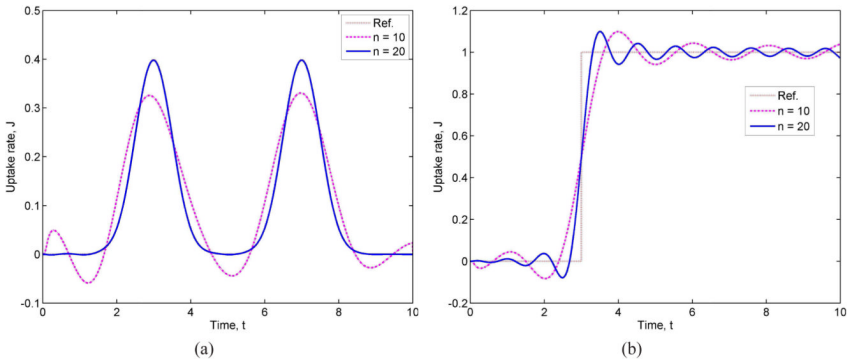

Figure 2.

Outputs for the basis function expansion approach for reference trajectories that are Gaussian [33] and step functions (for $D = v = 1$ and $k = 7.6$, which are the nondimensionalized parameters used for the entire paper). The number of basis functions is n and the number of eigenfunctions for the spatial variable was 10. The negative uptake rate is the result of a negative growth factor release, which is not physically realizable.

NIH-PA Author Manuscript
NIH-PA Author Manuscript
NIH-PA Author Manuscript

NIH-PA Author Manuscript

NIH-PA Author Manuscript

NIH-PA Author Manuscript

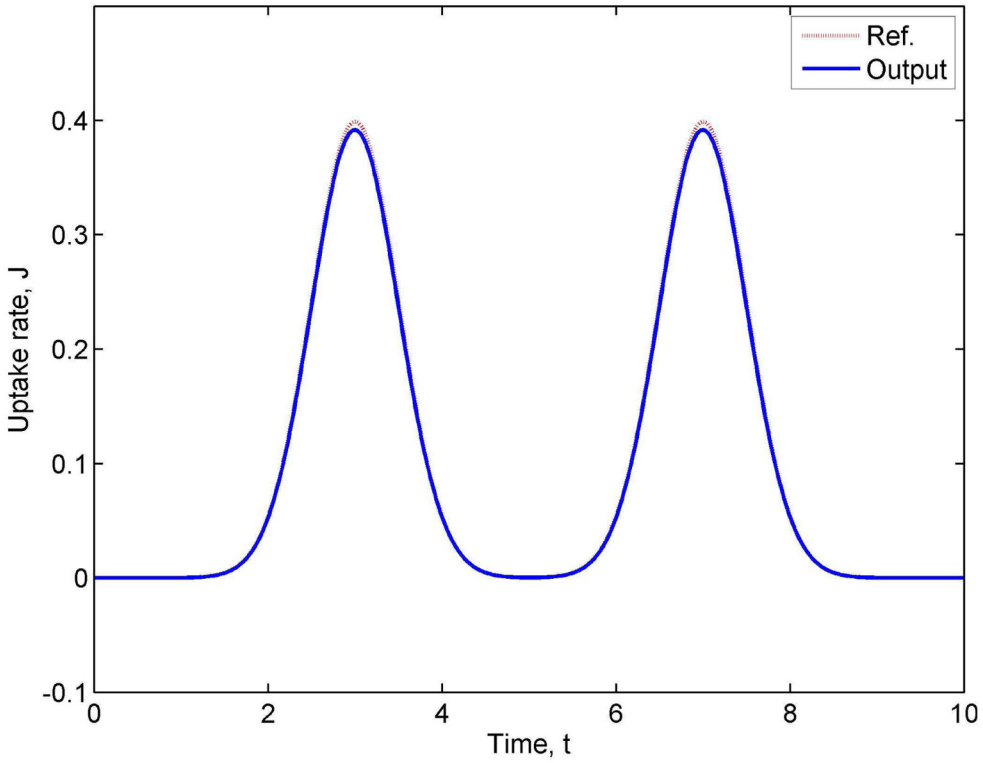

Figure 3.
Uptake rate using the method-of-moments approach. The number of Gaussians was $N = 2$.

NIH-PA Author Manuscript

NIH-PA Author Manuscript

NIH-PA Author Manuscript

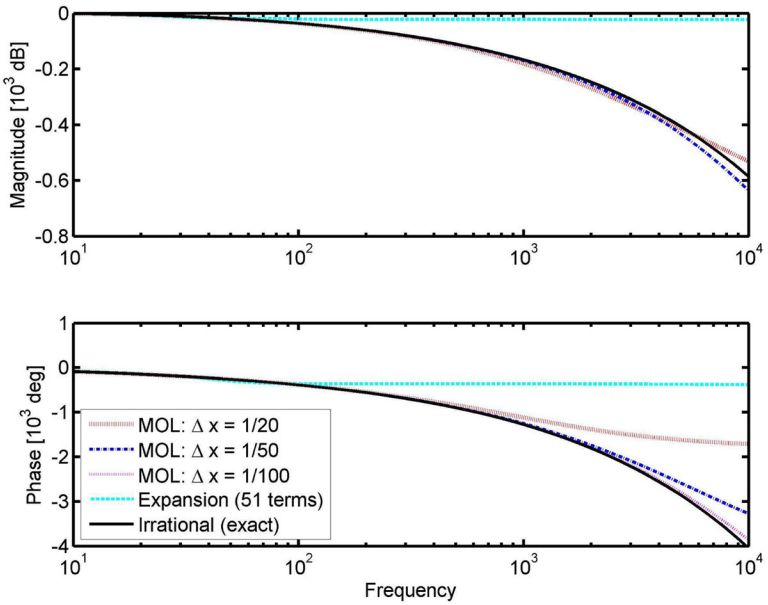

Figure 4.

Bode plots of various transfer functions. “MOL” corresponds to method of lines (34) with different discretization size, “Expansion” corresponds to (30), and “Irrational” corresponds to (22). The MOL magnitudes are within 10% of the exact solution for frequencies up to 10^3 (in dB), whereas the 51-term expansion can be 75% different from the exact solution.

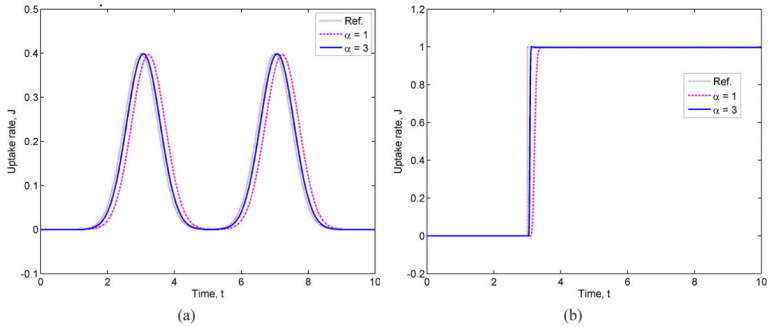

Figure 5.
Outputs obtained using the IMC approach with $\Delta x = 1/20$ and $\lambda = 0.0112174/\alpha$.

NIH-PA Author Manuscript
NIH-PA Author Manuscript
NIH-PA Author Manuscript

NIH-PA Author Manuscript
NIH-PA Author Manuscript
NIH-PA Author Manuscript

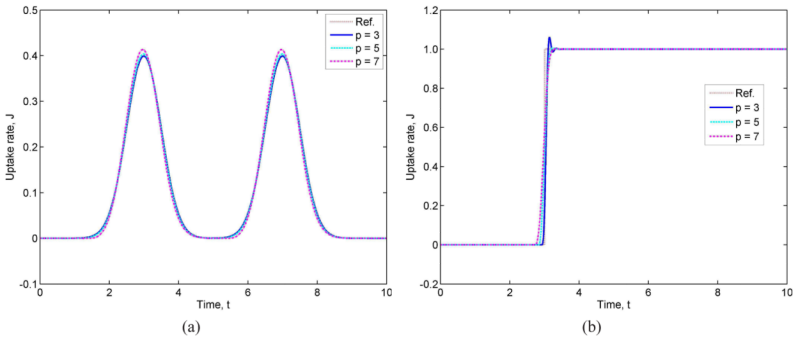

Figure 6.

MPC outputs for a control horizon of $m = 2$ and a sampling time $\Delta t = 1/10$ obtained for a state-space model obtained by the finite-difference method with $\Delta x = 1/20$. This sampling time corresponds to 100 seconds for a tissue thickness of 10^{-3} m and a diffusion coefficient of 10^{-9} m^2/sec.